LEVEL II

NUC TN 649

Copy

MOST ProJect -3

AN ACTIVE SONAR PERFORMANCE PREDICTION MODEL

by

W. H. Watson and R. W. McGirr

November 1971

NAVAL UNDERSEA RESEARCH AND DEVELOPMENT CENTER

San Diego, California 92132

⑥ AN ACTIVE SONAR PERFORMANCE PREDICTION MODEL

by

⑩ W. H. Watson and R. W. McGirr

⑫ 50 p.   ⑨ Technical notes

⑭ NUC-TN-649

⑪ November 1971

⑯ F11111

⑰ SF111111500

NAVAL UNDERSEA RESEARCH AND DEVELOPMENT CENTER
San Diego, California 92132

404 762

This technical note documents an active sonar performance prediction model developed at the Naval Undersea Research and Development Center. The primary application of this model is in predicting performance for surface ship sonar systems. This note is not to be considered an official NUC report.

PROBLEM

This report examines the problem of developing

Develop a high speed, compact performance prediction model for use in estimating operational performance of active, surface ship sonar systems. Such a model must be suitable for use on computers typically available at Navy laboratories and Fleet shore facilities.

RESULTS

An active sonar performance prediction model was developed. A concomitant computer program was written in FORTRAN IV and can provide detection outputs for a single system and environment in less than two minutes using a second generation computer, e.g., CDC 1604, IBM 7090, and UNIVAC 1230. This time is reduced by about one-tenth on newer machines, e.g., CDC 6500, IBM 360, and UNIVAC 1108.

RECOMMENDATIONS

Extend model applications by incorporating more sophisticated propagation loss prediction methods and higher order reverberation paths.

TABLE OF CONTENTS

ILLUSTRATIONS

I. INTRODUCTION

The Acoustic Environment Modeling Division, Code 506, of the Naval Under-
sea Research and Development Center (NUC), San Diego, California, has developed
a compact, high speed active sonar performance prediction model. This model
is a utility version of the Navy Interim Surface Ship Model[1] (NISSM).

Execution of the model is carried out with a computer program written
in FORTRAN IV. This computer program has a storage requirement of 16K 30-
bit words, and is operational on the UNIVAC 1230. It was developed for the
purpose of providing a fast program compact enough to run on available small
computers, but with sufficient accuracy to provide high confidence estimates
of operational sonar system performance.

This paper documents the mathematical and physical concepts contained
in the model. Certain sections of this report correspond closely to sections
of the NISSM report,[1] but have been included here for completeness. Most of
the computational effort required to implement the model is devoted to computing
propagation loss, reverberation level, and cumulative detection probability.

II. PROPAGATION LOSS

Propagation loss estimates are computed for near surface, bottom bounce,
and convergence zone paths. These paths are illustrated in FIG. 1.

A. Near Surface Propagation

The near surface propagation loss model is based on a set of ex-
pressions developed for NISSM.[1] This set of expressions consists
of the empirical AMOS[2] equations with the exceptions of modified surface
reflection loss and absorption loss expressions, and an added low frequency
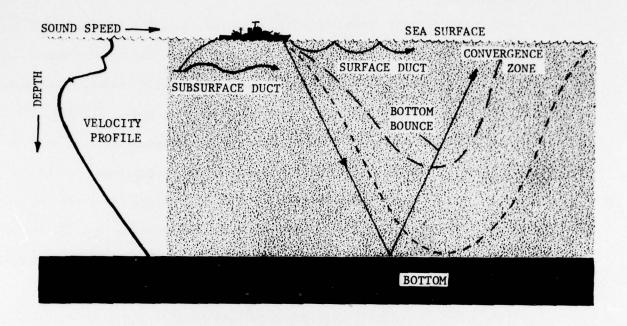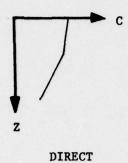
Figure 1. Propagation Paths
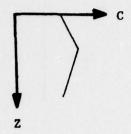
cutoff term. The AMOS expressions were primarily developed to predict surface duct and sub-surface duct propagation losses; however, their applicability has been extended to include direct path and double duct propagation loss predictions. Figure 2 shows the four near surface sound velocity profiles allowed. Each plot consists of straight line segments representing sound velocity C as a function of depth Z.

The AMOS equations can be expressed in terms of the following variables:
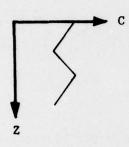
R - horizontal range (kyd)

Z_L - surface layer depth (ft)

2
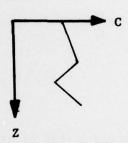
Figure 2. Near Surface Sound Velocity Profiles

Z_x - source depth (ft)

Z_t - target depth (ft)

f - frequency (kHz)

For convenience of expression the following scaled variables are introduced:

$$r = R/\sqrt{Z_L}$$

$$z_x = \sqrt{Z_x/Z_L}$$

$$z_t = \sqrt{Z_t/Z_L}$$

3

$$r_1 = \begin{cases} (1-z_x)/4 + (1-z_t)/4, & z_x \leq 1,\ z_t \leq 1, \\[2mm] (1-z_x)/4 + (\sqrt{z_t - 1})/5, & z_x \leq 1,\ z_t > 1, \\[2mm] (\sqrt{z_x - 1})/5 + (1-z_t)/4, & z_x > 1,\ z_t \leq 1. \end{cases}$$

When there is a surface duct the near surface propagation loss, H, is determined from the following set of equations.

1. <u>Direct Radiation Zone</u>. When $0 \leq r \leq r_1$ and both source and target depths are located within or at the bottom of the surface layer,

$$H = 60 + 20\log(R) + \alpha R + (r/r_1)G(z_t, z_x) \tag{1}$$

where α is the absorption coefficient in dB per kiloyard and

$$G(z_t, z_x) = \begin{cases} 0.1 \times 10^{2.3(z_t - z_x)}\,(f/25)^{1/3}, & z_t - z_x < 1 \\[2mm] 20(f/25)^{1/3}, & z_t - z_x \geq 1 \end{cases} \tag{2}$$

At all other times use the smaller of the two propagation losses computed by Eq. (1) and

$$H = 60 + 20\log(R) + \alpha R + [25 - \sqrt{|Z_x - Z_L|} - \sqrt{|Z_t - Z_L|} + 5R](f/25)^{1/3} \tag{3}$$

The quantity within brackets is taken as zero whenever negative.

4

2. <u>First-Order Surface Reflection and Shadow Zone.</u> When energy has been reflected at least once at the surface, corresponding to $r_1 \leq r \leq r_1 + 1/2$, the following equation is used

$$H = 60 + 20\log(R) + \alpha R + 2(r - r_1)K(z_t, z_x)$$

$$+ [1 - 2(r - r_1)]G(z_t, z_x) + N_{co} \qquad (4)$$

where

$$K(z_t, z_x) = 0.4C_f[10^{z_x} + 10^{z_t} + 10^{(z_t - z_x)}] \qquad (5)$$

with

$$C_f = \begin{cases} 1, & f \geq 8 \\ \\ (f/8)^{1/3}, & f \leq 8 \end{cases}$$

and N_{co} is the low frequency cutoff term described below. For this zone use either Eq. (3) or (4) whichever yields the smaller propagation loss.

3. <u>Second or Higher-Order Surface Reflection Zone.</u> When energy has been reflected at least twice at the surface, corresponding to $r > r_1 + 1/2$, the following equation is used

$$H = 60 + 10\log(R) + (\alpha + \alpha_s)R + K(z_t, z_x) - \alpha_s\sqrt{Z_L}(r_1 + 1/2)$$

$$+ 10\log[\sqrt{Z_L}(r_1 + 1/2)] + N_{co} \qquad (6)$$

5

where α_s is the surface reflection coefficient in dB per kiloyard. For this zone use either Eq. (3) or (6) whichever yields the smaller propagation loss.

4. <u>Subsurface Duct Propagation</u>. When subsurface duct conditions exist, as shown in FIG. 2, and both source and target are located within the bounds of the duct the following AMOS equation is used:

$$H = 60 + 20\log(R) + \alpha R + K(z_t', z_x') \qquad (7)$$

where

$$z_t' = \sqrt{2|Z_t - Z_a|/Z_a} ,$$

$$z_x' = \sqrt{2|Z_x - Z_a|/Z_a} ,$$

and Z_a is the depth of the axis of the subsurface duct (minimum sound speed depth) expressed in feet.

5. <u>Absorption Coefficient</u>. The absorption coefficient, α, is computed from a general purpose expression[3] that combines the low frequency predictions of Thorp[4] with the high frequency predictions of Schulkin and Marsh.[5] The resulting expression provides a best fit to existing data in the mid-frequency transition region. The absorption coefficient is

$$\alpha = \frac{1.776f^{1.5}}{32.768 + f^3} + \left(\frac{1}{1 + 32.768/f^3}\right)\left(\frac{0.65053f_T f^2}{f^2 + f_T^2} + \frac{0.026847f^2}{f_T}\right) \quad dB/kyd \quad (8)$$

where

$$f_T = 21.9 \times 10^{(30T + 102)/(5T + 2297)}$$

The term, f_T, is the relaxation frequency in kHz with temperature, T, expressed in °F. FIG. 3 shows α as a function of frequency for several average ocean temperatures computed by Eq. (8). A curve showing Thorp's[6] deep ocean predictions is presented for comparison.
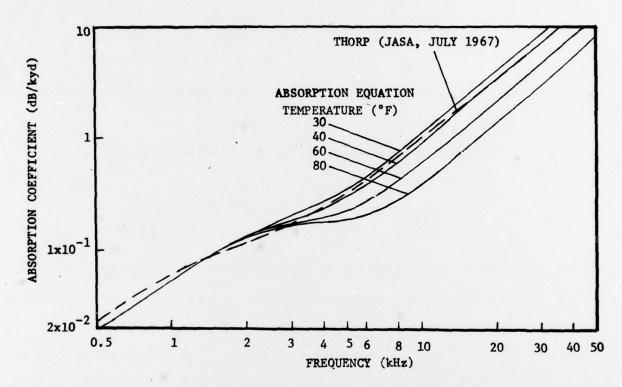
Figure 3. Absorption Coefficient vs Frequency (From Ref. 3)

6. _Surface Reflection Loss Coefficient_. The expression for the surface reflection loss coefficient, α_s, is given by

$$\alpha_s = \Gamma/R_b \quad \text{(dB/kyd)} \tag{9}$$

where Γ is the surface reflection loss per bounce, and R_b is the bounce distance corresponding to the range between surface contacts for the surface

7

duct limiting ray. According to findings of Schulkin and Marsh,[7] Γ exhibits a frequency-wave height product dependence given by

$$\Gamma = \begin{cases} 1.59\sqrt{fh}, & fh \geq 4.2691 \\ \\ 10 \log[1 + (fh/4.14)^4], & fh < 4.2691 \end{cases} \tag{10}$$

where f is the frequency in kHz and h is the mean crest-to-trough wave height in feet.

The bounce distance, $\tilde{R}_b$, is determined from

$$R_b = \sqrt{C_L^2 - C_s^2}/1500\gamma_o \qquad (kyd) \tag{11}$$

where C_L and C_s are the sound velocities, in ft/sec, at the layer depth and the surface, respectively, and γ_o is the sound velocity gradient, in ft/sec/ft, in the surface duct.

7. <u>Low Frequency Cutoff Term.</u> Arase and others[8-14] have reported the existence of low frequency cutoff in surface duct propagation.[1] This model incorporates an additive cutoff loss term based on an approximation to the normal mode surface duct model of Pedersen and Gordon.[9,10] The nth mode amplitude, A_n, is closely approximated by

$$A_n = U_n(t)U_n(t_o)e^{-1000\tau_n R}$$

where $U_n(t)$ and $U_n(t_o)$ are depth dependent functions of source and target depth, and τ_n is a mode damping factor given by

8
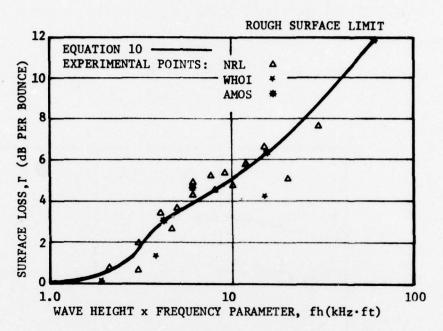
Figure 4. Surface Reflection Loss Curve (From Ref. 7)

$$\tau_n = (\pi f \gamma_o{}^2)^{1/3} \mathrm{Im}(Mx_n)/C_s$$

where $\mathrm{Im}(Mx_n)$ is the imaginary part of the nth eigenvalue. Assuming that the empirical AMOS equations correspond to the fully ducted normal mode situation, that $U_n(t)U_n(t_o)$ is a slowly varying function of frequency near cutoff, and that contributions from 2nd and higher order modes are negligible, the cutoff term can be expressed as
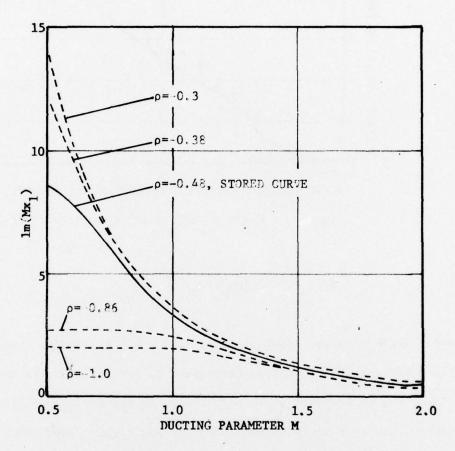
$$N_{co} = 20 \log(e^{-1000\tau_1 R}) \qquad \text{(dB)} \tag{12}$$

FIG. 5 shows the dependence of $\mathrm{Im}(Mx_1)$ on M and ρ. The parameters M and ρ are defined as

9

$$M = (8\pi^2 f^2 \gamma_o)^{1/3} z_L / c_s, \tag{13}$$

and

$$\rho = -|\gamma_o/\gamma_1|^{1/3}. \tag{14}$$

Figure 5. Imaginary Eigenvalues for First Mode

The quantity γ_1 is the below-layer sound velocity gradient in ft/sec/ft. Cutoff effects start near $M = 2.3$ and become extreme near $M = 1.0$.[10] A single curve corresponding to $\rho = -0.48$ is used in the model. Thus in

computing N_{co} the value for $Im(Mx_1)$ is obtained by computing M and then interpolating from a curve of $Im(Mx_1)$ versus M.

Propagation loss computations over a wide range of frequencies for three different layer depths are shown in FIG. 6. These computations were based on the (total energy) normal mode program of Watson and McGirr,[15] the NISSM program, and the FNWC approximate normal mode expression[11] as used in the SHARPS program. The results shown in FIG. 6 are normalized with respect to the FNWC maximum values to better display the relative cutoff effects. This comparison shows the FNWC cutoff is more gradual than the NISSM cutoff. However, this difference is expected since the FNWC cutoff uses an asymptotic approximation to $Im(Mx_n)$ that underestimates mode damping.
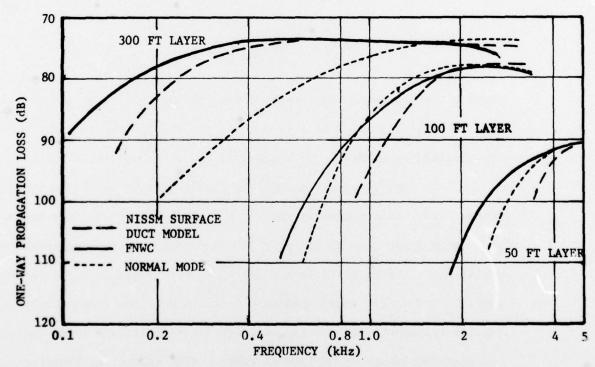
Figure 6. Surface Duct Cutoffs at 10 kyds Adjusted to FNWC Maximum Values (From Ref. 1)

B. Bottom Bounce and Convergence Zone Paths

One-way propagation loss for bottom bounce and convergence zone paths is given by

$$H = 60 + 20\log (S) + H_a + H_r + nH_b \qquad \text{(dB)} \qquad (15)$$

where S is slant range (kyd), H_a is absorption loss, H_r is refraction loss, H_b is bottom reflection loss, and n is the number of bottom reflections. For rays reflecting from the sea floor, bottom reflection loss, H_b, is obtained by interpolating from a curve of bottom reflection loss versus grazing angle.

1. Refraction Loss. Refraction loss, H_r, is determined from the expression[16-19]

$$H_r = 10\log \left[\frac{R \sin\phi_e}{S^2 \cos\phi_x} \left| \frac{dR}{d\phi_x} \right| \right] \qquad (16)$$

where ϕ_e is the angle the ray makes with the horizontal at end of trace, and ϕ_x is the ray angle at the source. The quantities R, S, and $dR/d\phi_x$ are obtained by means of ray tracing as described in the following section.

2. Ray Tracing. A complete family of rays is traced from source to sea floor, from source to sea surface, and from sea surface to target starting at a large depression angle ($\phi_x \simeq 90°$) and then incrementing toward smaller angles until the bottom limiting angle, $\phi_L = \text{Arccos}(C_x/C_b)$, is reached, where C_x and C_b are sound speeds at source and bottom respectively. The angular increments are successively modified to maintain approximately constant increments in horizontal range. When the bottom limiting angle has been reached the bottom bounce computations are complete and convergence

zone computations are initiated. The angular interval obtained by taking the difference between the bottom limiting angle, ϕ_L, and the surface duct limiting angle, $\phi_d = \text{Arccos}(C_x/C_L)$, is divided into twenty equal increments. Then starting at ϕ_d, ray tracing is carried out in a manner similar to that used in the bottom bounce computations until the bottom limiting angle is reached.

All ray path parameters needed to compute refraction loss are computed for each ray. These parameters include horizontal range, R, slant range, S, path time, T, and the derivative of horizontal range with respect to initial depression angle, $dR/d\phi_x$.

Ray paths from source to bottom, from source to surface, and from surface to target are generated by combining the various ray path components. The basic ray trace components involved are outlined in FIG. 7.
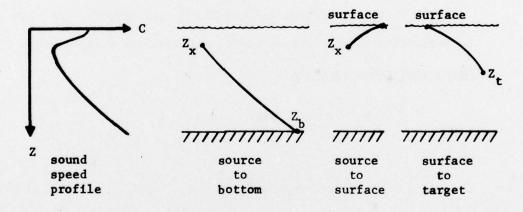
Figure 7. Computed Ray Path Components

The raytrace technique uses a constant sound speed gradient approximation to the actual sound speed profile as shown in FIG. 8. This

13

profile approximation allows ray tracing through constant gradient layers.[20,21]
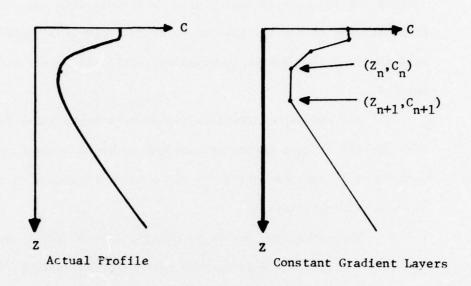
Figure 8. Sound Speed Profile Approximation

The following incremental quantities are computed for each layer, where by definition the nth layer extends between interfaces n and $n + 1$:

horizontal range increment

$$\Delta R_n = (C_v/\gamma_n)(\sin\phi_n - \sin\phi_{n+1}) \qquad (17)$$

where

$$C_v = C_n/\cos\phi_n, \text{ and}$$

$$\gamma_n = (C_{n+1} - C_n)/(Z_{n+1} - Z_n).$$

slant range increment

14

$$\Delta S_n = (C_v/\gamma_n)(\phi_n - \phi_{n+1}) \qquad \text{(ft)} \qquad (18)$$

travel time increment

$$\Delta T_n = \frac{1}{\gamma_n} \ln \left[\frac{C_{n+1}}{C_n} \quad \frac{1 + \sin\phi_n}{1 + \sin\phi_{n+1}} \right] \qquad \text{(sec)} \qquad (19)$$

derivative increment

$$\Delta \left(\frac{dR}{d\phi_x} \right)_n = \frac{C_v}{\gamma_n} \tan \left[\frac{1}{\sin\phi_n} - \frac{1}{\sin\phi_{n+1}} \right] \qquad \text{(ft/radian)} \qquad (20)$$

These equations hold as long as $\gamma_n \neq 0$, $\phi_n \neq 0$ and $\phi_{n+1} \neq 0$. When $\gamma_n = 0$ the following expressions are used

$$\Delta R_n = \Delta z_n \cot\phi_n, \text{ with } \Delta Z_n = Z_{n+1} - Z_n,$$

$$\Delta S_n = \Delta z_n / \sin\phi_n,$$

$$\Delta T_n = \Delta S_n / c_n, \text{ and}$$

$$\Delta \left(\frac{dR}{d\phi_x} \right)_n = \frac{\Delta R_n}{\sin\phi_n \sin\phi_{n+1}} \ .$$

When vertexing occurs within the nth layer ($\phi_{n+1} = 0$) the expression for the derivative becomes

$$\Delta \left(\frac{dR}{d\phi_x} \right) = \frac{c_v/\gamma_n}{|\sin\phi_n|}$$

The final values in the appropriate units are obtained by summing the increments over the ray path to give

$$R = \frac{1}{3000} \Sigma \ \Delta R_n \qquad\qquad \text{(kyd)},$$

$$S = \frac{1}{3000} \Sigma \ \Delta S_n \qquad\qquad \text{(kyd)},$$

$$T = \Sigma \ \Delta T_n \qquad\qquad \text{(sec)},$$

and $\qquad \dfrac{dR}{d\phi_x} = \dfrac{1}{3000} \Sigma \ \Delta\left(\dfrac{dR}{d\phi_x}\right)_n \qquad$ (kyd/radian).

III. MASKING BACKGROUND

The total masking background is comprised of both reverberation and noise. Masking level, M, may be computed as the incoherent addition of noise and reverberation components, that is:

$$M = 10 \ \log \left[10^{N/10} + 10^{R_t/10} \right] \quad \text{(dB re 1 } \mu\text{bar)} \qquad (21)$$

where N is total noise level in the input band in dB//1µbar, and R_t is total reverberation in the input band in dB//1µbar.

A. Noise Level

Assuming a constant noise spectrum level over the input band, the total noise band level can be expressed as follows:

$$N = N_s - D + 10 \log(\Delta f) \qquad (dB/re \ 1 \ \mu bar) \qquad (22)$$

where N_s is the isotropic noise spectrum level in dB/re 1 μbar, D is the directivity index in dB, and Δf is the bandwidth in Hz.

1. <u>Spectrum Level and Bandwidth</u>. The isotropic noise spectrum level, N_s, is assumed to be independent of range. Typically it depends on platform speed, sea state, and frequency.[22]

2. <u>Directivity Index</u>. An approximate expression based on horizontal and vertical beamwidths is used to compute directivity index. The beamwidths $\Delta\theta$ and $\Delta\phi$ are assumed to represent effective receiving array values. FIG. 9 illustrates the equivalent three dimensional beam defined by these parameters.
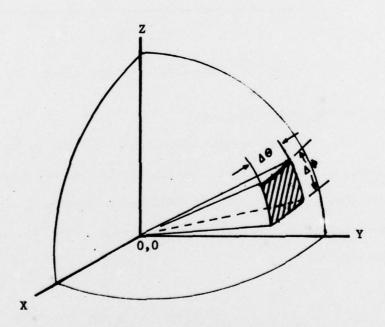
Figure 9.   Beam Configuration for Directivity Index
Computation

17

Assuming unity response over the surface area defined by $\Delta\theta\Delta\phi$, and zero elsewhere, the directivity index, D, can be approximated by

$$D \simeq 10 \log\left(\frac{4\pi}{\Delta\theta\Delta\phi}\right) \tag{23}$$

where $\Delta\theta$ is the horizontal half power beamwidth in radians and $\Delta\phi$ is the vertical half power beamwidth in radians. FIG. 10 illustrates the directivity index as given by eq. (23) as a function of $\Delta\phi$ for a fixed value of $\Delta\theta$.
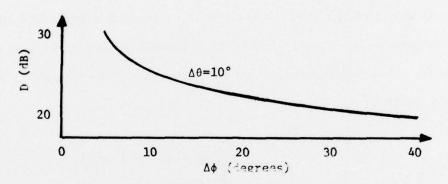
Figure 10. Directivity Index versus Half-Power Beamwidth

B. Reverberation Level

The total reverberation level is taken to be the resultant of bottom, volume, and surface reverberation levels obtained from downgoing ray paths and, when a duct exists, the additional volume and surface reverberation levels from surface duct paths. Thus, the total reverberation level, R_t, may be expressed as

$$R_t = 10 \log\left[10^{R_b/10} + 10^{R_v/10} + 10^{R_s/10} + 10^{R_v^d/10} + 10^{R_s^d/10}\right] \tag{24}$$

18

where

R_b is bottom reverberation level via deep ocean paths (dB),

R_v is volume reverberation level via deep ocean paths (dB),

R_s is surface reverberation level via deep ocean paths (dB),

R_v^d is volume reverberation level via surface duct (dB), and

R_s^d is surface reverberation level via surface duct (dB).

These reverberation paths are illustrated in Fig. 11.
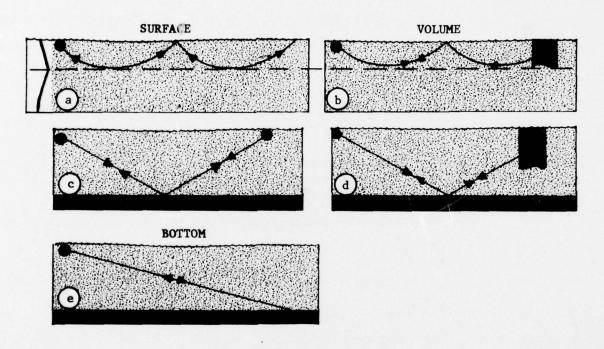
Figure 11. Reverberation Paths

The computational scheme involves using previously computed ray parameters for a sequence of source ray angles. The reverberation values (not including system corrections) are computed and stored as functions of travel time for each defined reverberation path. In the final computations

19

for each mode the reverberation values are obtained by interpolating from the previously stored reverberation values using the appropriate echo travel times. Travel time as a function of horizontal range is computed from $T = C_s/R$ for the surface duct case and from the stored target ray path parameters for the bottom bounce and convergence zone modes. System parameter corrections for source level, lobe shapes, and pulse length are then made in order to arrive at the input band reverberation level.

1. <u>Basic Reverberation Expression</u>. The general expression for each reverberation component, R_k, is

$$R_k = I_o + B_k(\phi_x) + B_k(\phi_r) - 2H_k + 10 \log(S_k) + 10 \log(A_k) \quad (dB) \quad (25)$$

where I_o is intensity level along main lobe axis (dB re 1 μbar at 1 yd from array,

$B_k(\phi_x)$ is array response correction for transmitting rays to the kth surface (dB),

$B_k(\phi_r)$ is array response correction for receiving rays from the kth surface (dB),

H_k is one way propagation loss to the kth scattering surface (dB),

$10 \log(S_k)$ is scattering strength at the kth surface (dB/sq yd), and

A_k is effective scattering area of kth surface (sq yd).

Equation (25) is applicable to all reverberation paths since volume scattering strength is expressed in terms of area of scattering water column.

2. <u>Array Response Corrections</u>. Array response corrections are required for both echo and reverberation paths. In the horizontal plane no array corrections are necessary since all echo and reverberation returns intercept the beam pattern along the horizontal projection of the main lobe axis. In the vertical plane, however, response corrections are necessary since echo and reverberation returns can arrive over a wide range of depression angles (see Fig. 12).

The array correction technique assumes that the target is being tracked by the horizontal beam and that only vertical deviation loss occurs for target and reverberation rays. Two alternative methods are available for computing vertical main lobe response. One method allows interpolation from a curve of response versus depression angle, whereas the other approach approximates the main lobe response by a $\sin(x)/x$ function.
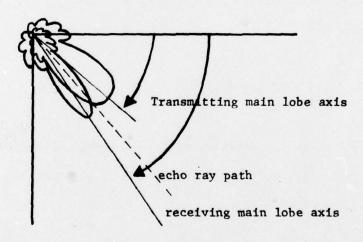
Figure 12. Ray Paths Intercepting Vertical Array Patterns

Assuming unity response on the main lobe, the response correction for a given depression angle ϕ can be written as

21

$$B(\phi) = 20 \log \left[\frac{\sin(k|\phi - \phi_o|)}{k|\phi - \phi_o|} \right]$$

where ϕ is ray depression angle, and ϕ_o is main lobe depression angle.

Let $\Delta\phi$ represent the vertical, half-power beamwidth, then the value of k is determined by setting $B(\phi) = 3$ dB and $|\phi - \phi_o| = \Delta\phi/2$. Thus,

$$\frac{\sin(x)}{x} = 0.707,$$

where

$$x = k\Delta\phi/2.$$

A numerical solution yields $x = 1.41$, so that $k = 2.82/\Delta\phi$. The final expression is

$$B(\phi) = 20 \log \left[\sin(\frac{2.82}{\Delta\phi} |\phi - \phi_o|) \right] . \quad \text{(dB)} \quad\quad (26)$$

Figure 13 shows how the $\sin(x)/x$ function represents vertical lobe shapes for two steering angles $\phi_o = 0°$ and $\phi_o = 20°$, and for beamwidths of $\Delta\phi = 10°$ and $\Delta\phi = 6°$, respectively.

3. _Reverberation Propagation Losses_. The propagation loss for the various reverberation paths is computed using the surface duct, bottom bounce and convergence zone propagation loss expressions described earlier. The

22

B(φ)

φ=0°

Δφ=10°

φ_o=20°

Δφ=6°

Beam Pattern Response (dB)

Ray Depression Angle (degrees)
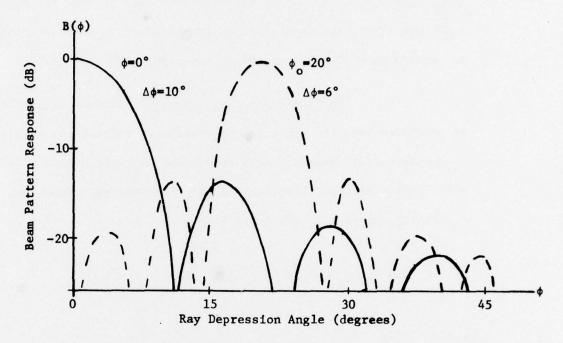
Figure 13. Vertical Array Correction Parameters

propagation loss to the target is used to compute volume reverberation
via the bottom path since the interfacing scatterers must be near the
target.

In computing surface duct reverberation the surface component of
reverberation is obtained by setting the target depth, Z_t, to zero. The
volume component is obtained by setting $Z_t = Z_L/3$; a value selected to
approximate the effective depth of scatterers within the duct.

4. _Scattering Strengths_. Scattering strengths are required for
surface, volume, and bottom reverberation predictions. Analytical expressions
are used for computing surface and bottom scattering strengths, but volume

23

scattering strength is provided as a program input. Since little is known about the depth distribution of scatterers, and because of existing measurement techniques, volume scattering is expressed in terms of scattering strength per square yard of water column at one yard.[23],[24]

a. <u>Surface Scattering Strength</u>. Surface scattering strength is predicted from the empirical expression of Chapman and Harris.[25] Let ϕ_s denote surface grazing angle in degrees, v_w denote wind speed in knots, and f denote acoustic frequency in kHz, then the expression for surface scattering strength in dB/yd^2 at 1 yard is

$$10 \log S_s = 3.3\beta \ln(\phi_s/30) - 42.4 \ln\beta + 2.6 \tag{27}$$

where

$$\beta = 158(v_w f^{1/3})^{-0/58}.$$

FIG. 14 shows typical curves of $10 \log S_s$ vs ϕ_s at three values of wind speed for a representative active sonar frequency of 3.5 kHz.
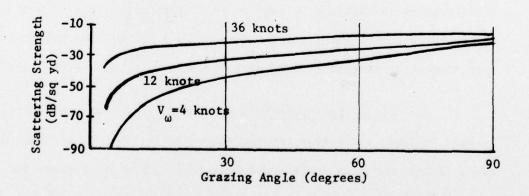
Figure 14. Surface Scattering Strength vs Grazing Angle
(From Ref. 26)

24

b. <u>Bottom Scattering Strength</u>. The expression for bottom scattering strength takes into consideration diffuse scattering at small angles in accordance with Lambert's law[27] and specular scattering at large angles.[28] The resulting expression for scattering strength in dB per square yard at 1 yard is

$$10 \log S_b = 10 \log \left[\mu_b \sin^2 \phi_b + \exp(-100 \cot^2 \phi_b) \right] \qquad (28)$$

where μ_b is the bottom diffusion constant, and ϕ_b is the bottom grazing angle in degrees.

The constant 100 appearing in the specular reflection term provides an approximate fit to data obtained from experiments in the Norwegian Sea.[1,29] Figure 15 shows $10 \log S_b$ vs ϕ_b for the case $\mu_b = 0.002$.
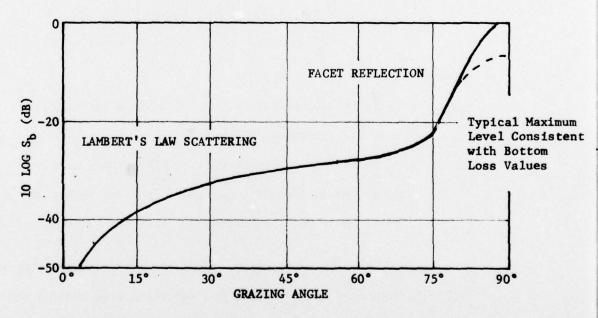
Figure 15. Bottom Scattering Strength

As ϕ_b approaches 90° (normal incidence) the specular term becomes dominant and tends to predict excessive backscattering. To avoid this over-prediction the value obtained from the above expression is made to be consistent with the assumed bottom type by limiting the backscattering level to the value predicted by using near normal incidence bottom reflection loss values. This effect is shown in FIG. 15 as the dashed curve when the grazing angle approaches 90°.

5. <u>Scattering Area</u>. Since volume scattering is measured with respect to the effective scattering water column, all backscattering levels are expressed in terms of a scattering area; consequently, a general expression for scattering area may be used. The effective scattering area of the kth scattering surface, A_k, is given by

$$A_k = (1/2 \ c_k \tau/\cos\phi_k) \ R_k \Delta\Theta \qquad (29)$$

where

c_k is the sound velocity at k^{th} surface (ft/sec),

τ is the pulse length (sec),

ϕ_k is the intercepting angle at k^{th} surface (degrees),

R_k is the horizontal range to k^{th} surface (kyd), and

$\Delta\Theta$ is the effective horizontal half-power beamwidth (radians).

Special care must be taken in equation (29) as ϕ_b approaches 90°. In this case $\cos\phi_b \to 0$ and the resulting area becomes unbounded. This situation is remedied by limiting the maximum bottom surface scattering area to a value predicted by

26

$$A_k = Z_b \Delta\phi_r R_k \Delta\Theta \qquad (30)$$

where Z_b is the bottom depth in feet and $\Delta\phi_r$ is the receiving vertical half-power beamwidth in radians.

Figure 16 shows the defining geometry for the bottom path, where for this case $c_k = c_b$ and $\phi_k = \phi_b$.
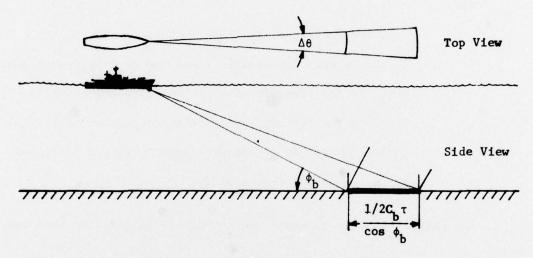
Figure 16. Area Description for Bottom Reverberation

The separation of the area-defining rays has been exaggerated for the purpose of illustration. In all reverberation computations in this model the location of the scattering surface is assumed to be defined by a single ray with its associated source angle, range to scattering surface, and propagation loss. This simplified computational technique is assumed adequate for Fleet sonar systems since typical raytrace range resolutions are suf-ficiently high to support the single ray assumption.

27

IV. SIGNAL TO NOISE RATIO

The signal to noise ratio or, specifically, the echo to masking background in the input band is a critical detection quantity. The echo signal level is computed from the expression

$$E = I_o + B(\phi_x) + B(\phi_r) - 2H_t + S_t \qquad (31)$$

where

E is the echo level in dB re 1 μbar,

I_o is the main lobe source level (dB re 1 μbar at 1 yd),

$B(\phi_x)$ is the transmit beam pattern correction (dB),

$B(\phi_r)$ is the receive beam pattern correction (dB),

H_t is the one way propagation loss to target (dB), and

S_t is the target strength (dB).

The signal to noise (masking background) ratio in dB is then computed from

$$(S/N) = E - M, \qquad (dB)$$

and is used in obtaining detection probability.

V. DOPPLER GAIN

In many ASW engagements target doppler can be a determining factor in target detectability. Essentially doppler shifts the desired echo out of the reverberation frequency band. Under reverberation limiting conditions the net effect is an increase in signal-to-reverberation level.

28

An approximate model is used for estimating doppler gain as a function of closing speed and the pertinent system parameters. The doppler gain model is based on the simple physical picture of a signal being shifted out of the reverberation frequency band. Echo and reverberation intensities are arbitrarily represented by a Gaussian distribution with standard deviation $1/\tau$.

Figure 17A shows reverberation response as a function of frequency for a tone pulse transmitted at f_o. The cross sectioned area is the reverberation energy, $R_v(0)$, falling within the signal bandwidth.

Figure 17C shows an assumed echo spectrum which has been doppler shifted by Δf determined from[30]

$$\Delta f = 0.7 \ fV_c \qquad \text{(Hz)} \qquad (32)$$

where V_c is the closing speed in knots. The reverberation energy falling within the echo band under these conditions is given by the cross sectioned area of FIG. 17B denoted by $R_v(\Delta f)$. The resulting doppler gain, G_d, due to increased signal-to-reverberation level may be expressed as

$$G_d = 10 \ \log \left(\frac{E_1/R_v(\Delta f)}{E_1/R_v(0)} \right) \qquad \text{(dB)} \qquad (33)$$

where E_1 is the echo energy in the signal band in units compatible with R_v. Since the total signal energy, E_1, is assumed to be constant, equation (33) can be written as

$$G_d = 10 \ \log \left(\frac{R_v(0)}{R_v(\Delta f)} \right) \qquad \text{(dB)} \qquad (34)$$

29
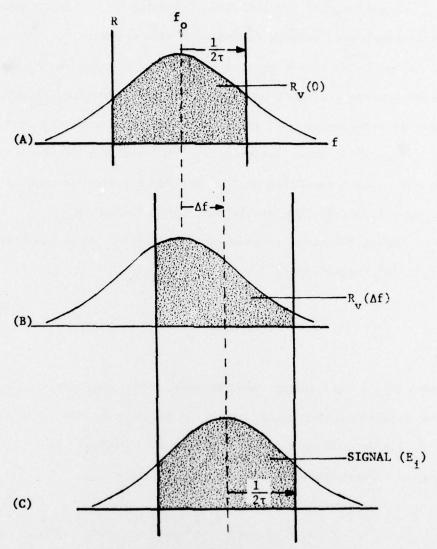
Figure 17. Doppler Gain Model

Using the standardized normal distribution function defined by

$$\Phi(x) = (1/\sqrt{2\pi}) \int_{-\infty}^{x} \exp(-y^2/2)\,dy, \tag{35}$$

the reverberation energy values are determined from

30

$$R_v(0) = 2\Phi(1) - 1 = 0.68, \text{ and} \tag{36}$$

$$R_v(\Delta f) = \Phi(2\tau\Delta f + 1) - \Phi(2\tau\Delta f - 1). \tag{37}$$

Thus

$$G_d = 10 \log \left[\frac{0.68}{\Phi(2\tau\Delta f + 1) - \Phi(2\tau\Delta f - 1)} \right] . \tag{38}$$

Figure 18 is a plot of G_d as a function of Δf. Doppler gain is incorporated into the computations as a net reduction in total reverberation using

$$R_t' = R_t - G_d$$

where R_t' is the doppler corrected reverberation level in the signal band. A practical limit to the doppler gain occurs when R_t' is reduced to the noise level since the system is then no longer reverberation limited.

While the doppler calculation described above is approximate it does provide a mechanism for incorporating the general effects of doppler gain. This doppler model was not developed for a particular system configuration; consequently, it may be used for various system designs and detection schemes.

VI. DETECTION PROBABILITY

Two types of detection probability are required to provide a measure of system performance. One is the single ping detection probability and and the other is the cumulative detection probability. The single ping

31
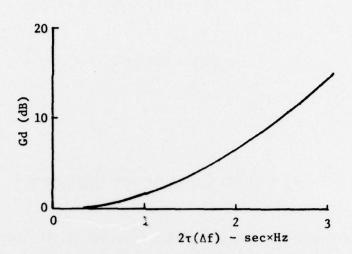
Figure 18.   Reverberation Doppler Gain vs Doppler
Frequency Shift

value provides the probability that a single target echo from a given trans-
mission will be detected from the masking background. The cumulative quantity
provides the probability that three or more echos will be detected from
sequential groups of five consecutive transmissions.

For the near surface path the fifty percent single ping probability has
found extensive application in predicting detection range. For cases where
the single ping probability rises rapidly toward unity and remains high for
several transmissions the single ping value provides a suitable detection
range estimate. In contrast, erroneous detection ranges may result from
using the fifty percent single ping criteria for situations involving a
detection annulus or zone, or for cases where the probabilities increase slowly
and sustain levels slightly less than fifty percent.

Operationally, a target detection requires more than one echo return and
is therefore a function of the number of pings involved. Specifically,

detection depends on interpulse period, closing speed, and detection annulus width. Generally, the two-out-of-four or the three-out-of-five echo to ping criteria have been accepted as valid measures of operational detection range. This prediction model incorporates a cumulative detection probability scheme based on a three or more out of five criterion. The resulting detection quantities provide detection range estimates for most operational situations.

A. Single Ping Detection Probability

For an assumed log-normal distribution of signal excess, the single ping probability of detection, p, can be written as

$$p = \Phi \left(\frac{(S/N) - N_{rd}}{\sigma} \right) \tag{39}$$

where N_{rd} is the recognition differential in dB (input signal to noise ratio for fifty percent probability of detection), and σ is the standard deviation of (S/N) in dB. The function Φ is the standardized normal distribution function defined in equation (35).

B. Cumulative Detection Probability
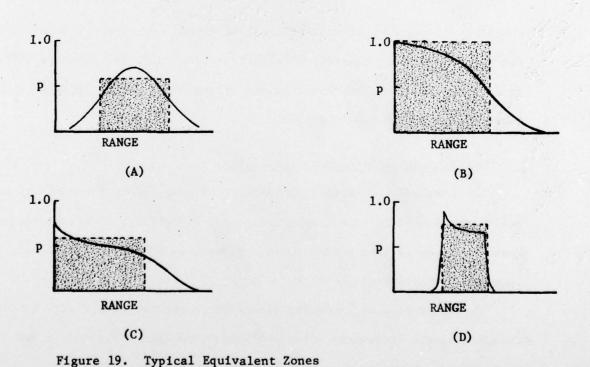
Cumulative detection probability is computed on the basis of an equivalent detection zone having a constant probability. This equivalent detection zone is then used with the expressions of Arndt[31] to compute the required probabilities.

The first step in computing cumulative detection probability involves determining the equivalent detection zone. The zone threshold is set equal to half the maximum value of single ping probability of detection. The

33

equivalent zone is then defined by the ranges where the single ping probability curve crosses this threshold. The average signal to noise ratio over the equivalent zone is then computed from

$$(\overline{S/N}) = \sum_{i=1}^{K} \frac{(S/N)_i}{K} \qquad (40)$$

where $(\overline{S/N})$ is the mean signal to noise ratio over the equivalent zone, and K is the total number of samples existing through the zone. The value of $(\overline{S/N})$ is then used with the standardized normal distribution function to compute $\overline{p}$. Figure 19 illustrates the character of equivalent zones applicable to several situations. The solid line denotes the original p function while the shaded region is the equivalent zone at a level of $\overline{p}$.

Figure 19. Typical Equivalent Zones

Following Arndt, an expression for the cumulative probability of the kth sample, P_k, can be written recursively as

$$P_{k+1} = P_k + (1 - P_k) \left[\frac{s_k}{s_k + f_k} \right] \overline{p} \tag{41}$$

where s_k is the probability that the kth group of samples is within one of success, and f_k is the probability that the kth group is not within one of success and none of the group has contributed to an earlier success.

For the case of three or more pings from a group of five, the following closed form expressions for s_k and f_k (see eq. (41)) are used.

i	s_k	f_k
1	0	0
2	0	0
3	p^2	0
4	$3p^2q$	$q^3 + 3pq^2$
5	$6p^2q^2$	$q^4 + 4pq^3$
6	$6p^2q^3$	$q^5 + 5pq^4 + 4p^2q^3$
7	$5p^2q^4 + 3p^3q^3$	$q^6 + 6pq^5 + 9p^2q^4 + 2p^3q^3$
8	$6p^2q^5 + 8p^3q^4 + p^4q^3$	$q^7 + 7pq^4$
9	$6p^2q^6 + 14p^3q^5 + 6p^4q^4$	$q^8 + 8pq^6 + 14p^2q^5$

Note that $q = 1 - p$.

The final cumulative detection probability is computed by selecting a series of samples from the equivalent zone. These samples start at the maximum equivalent zone range and are spaced at interpulse intervals defined by

$$\Delta R = 0.000563 \, V_c T \qquad \text{(kyd)}$$

where T is the time between pings in seconds. The resulting series of K
samples of constant probability $\bar{p}$ is then used with the cumulative probability
expressions to compute the cumulative probability of detection versus range.

GLOSSARY OF TERMS

Symbol	Definition
A_k	effective scattering area of the kth surface (yd^2)
A_n	n^{th} mode amplitude term in the normal mode surface duct solution
α	absorption coefficient (dB/kyd)
α_s	surface reflection coefficient (dB/kyd)
$B(\phi)$	array response corrections at depression angle ϕ (dB)
C_b	sound speed at bottom depth (ft/sec)
C_k	sound speed at k^{th} scattering surface (ft/sec)
C_L	sound speed at layer depth (ft/sec)
C_s	sound speed at surface (ft/sec)
C_v	sound speed at vertex depth (ft/sec)
C_x	sound speed at source depth (ft/sec)
C_n	sound speed at n^{th} depth in sound speed profile array
C_f	frequency switch function
D	directivity index (dB)
Δ	increment or forward difference operator
Δf	bandwidth (Hz)
E	echo level (dB re 1 μbar)
E_1	echo energy in the signal band
f	acoustic center frequency
$G(z_t, z_x)$	depth loss factor in AMOS equations (dB)
G_d	doppler gain (dB)

37

Symbol	Definition
Γ	surface reflection loss per bounce (dB/kyd)
γ_o	in-layer sound speed gradient (ft/sec/ft)
γ_1	below-layer sound speed gradient (ft/sec/ft)
γ_n	sound speed gradient in n^{th} segment of sound speed profile
H	total one-way propagation loss (dB)
H_a	absorption loss (dB)
H_r	refraction loss (dB)
H_b	bottom reflection loss (dB)
H_k	one-way propagation loss to the kth scattering surface (dB)
h	mean crest-to-trough wave height (ft)
$Im(Mx_n)$	imaginary part of the nth eigenvalue associated with the normal mode surface duct solution
I_o	intensity level along main lobe axis (dB at yd re 1 μbar)
$K(z_t, z_x)$	depth loss factor in AMOS equations (dB)
M	ducting parameter, or masking background
N	number of bottom reflections, or total noise level in the input band (dB)
N_{co}	cut off loss (dB)
N_s	isotropic noise spectrum level (dB re 1 μbar)
Φ	standard normal distribution function
ϕ	ray depression angle
ϕ_e	angle ray makes with horizontal at end of trace
ϕ_x	angle ray makes with horizontal at source
ϕ_L	bottom limiting angle
ϕ_o	main lobe depression angle

Symbol	Definition
ϕ_s	surface grazing angle
R	horizontal range (kyd)
r	normalized range used in AMOS equations
r_1	normalized first bounce distance
R_b	bounce distance (kyd)
R_t	total reverberation level in input band (dB)
R_t'	total reverberation level in doppler signal band (dB)
R_b	bottom reverberation level via deep ocean path (dB)
R_v	volume reverberation level via deep ocean path (dB)
R_s	surface reverberation level via deep ocean path (dB)
R_v^d	volume reverberation level via surface duct (dB)
R_s^d	surface reverberation level via surface duct (dB)
R_k	reverberation component to the kth scattering surface (dB)
$R_v(\Delta f)$	reverberation energy falling in the echo band with doppler shift Δf
ρ	parameter associated with normal mode surface duct solution
S	slant range (kyd)
S_k	scattering strength at the kth surface
S_s	surface scattering strength
S_t	target strength (dB)
(S/N)	signal-to-noise ratio
T	ray path travel time (sec) or time between pings (sec)
τ	signal pulse length (sec)
τ_n	n^{th} mode damping factor

Symbol	Definition
$U_n(t)$	depth loss factor associated with the normal mode surface duct solution
V_c	closing speed (knots)
V_w	wind speed (knots)
Z_b	bottom depth (ft)
Z_L	layer depth (ft)
Z_t	target depth (ft)
Z_x	source depth (ft)
Z_n	n^{th} depth in sound speed profile array
z_t	normalized target depth (AMOS)
z_x	normalized source depth (AMOS)

REFERENCES

1. Naval Ship Systems Command. First Summary Report, Navy Interim Surface
   Ship Sonar Prediction Model (NISSM) (U), by Ad Hoc Committee on Sonar Model
   Standards (COSMOS). April 1971, CONFIDENTIAL.

2. U. S. Naval Underwater Sound Laboratory. Report 255A, Report on the Status
   of Project AMOS (Acoustic, Meteorological and Oceanographic Survey), 1 Jan
   1953-31 Dec 1954, by H. W. Marsh, M. Schulkin. 23 March 1955, revised 9 May
   1967.

3. H. R. Hall, W. H. Watson. A New Absorption Coefficient Expresssion for Use
   in Sonar Range Prediction (U). U. S. Navy J. Underwater Acoustics 17:617-637,
   October 1967, CONFIDENTIAL.

4. W. H. Thorp. Deep-Ocean Sound Attenuation in the Sub- and Low-Kilocycle-
   per-Second Region. J. Acoust. Soc. Amer. 38:648-654, October 1965.

5. M. Schulkin, H. W. Marsh. Sound Absorption in Sea Water. J. Acoust. Soc.
   Amer. 34:864-865, June 1962.

6. W. H. Thorp. Analytic Description of the Low-Frequency Attenuation Co-
   efficient. J. Acoust. Soc. Amer. 42:270, July 1967.

7. M. Schulkin, H. W. Marsh. The Effect of Ocean Scattering on the Propagation
   of Underwater Sound. U. S. Navy J. Underwater Acoustics 10:293-300, April
   1960.

8. T. Arase. Some Characteristics of Long Range Explosive Sound Propagation.
   J. Acoust. Soc. Amer. 31:588-594, May 1959.

9. M. A. Pedersen, D. F. Gordon. Normal-Mode Theory Applied to Short-Range
   Propagation in an Underwater Acoustic Surface Duct. J. Acoust. Soc. Amer.
   37:105-118, January 1965.

10. U. S. Navy Electronics Laboratory. Report 1407, Normal Mode Approach to
    Underwater Sound Propagation (U), by M. A. Pedersen, D. F. Gordon, 27 September
    1966, CONFIDENTIAL.

11. C. S. Clay. Sound Transmission in a Half Channel and Surface Duct, Meteorology
    International Incorporated, Project M-153, Technical Note Two 2:1-17, August
    1968.

12. W. H. Furry. Theory of Characteristic Functions in Problems of Anomalous
    Propagation. Mass. Inst. Technology Laboratory Report 680, 1945: Methods
    of Calculating Characteristic Values for Bilinear M Curves, ibid Report 795,
    1946.

13. U. S. Naval Underwater Sound Laboratory. Report 111, Theory of the Anomalous
    Propagation of Acoustic Waves in the Ocean, by H. W. Marsh, 1950.

14. Naval Undersea Warfare Center. Technical Paper 107, Underwater Sound Propagation in the Three-Layer Ducts Computed by Normal Modes, by D. F. Gordon, R. F. Hosmer, December 1968.

15. U. S. Navy Electronics Laboratory. Technical Memorandum 921, A Surface Channel Propagation Loss Model I, by W. H. Watson, R. W. McGirr, 30 May 1966.

16. J. W. Horton. Fundamentals of Sonar, U. S. Naval Institute, Annapolis, Md., 1957, pp. 99-101.

17. C. B. Officer. Introduction to the Theory of Sound Transmission, McGraw-Hill Book Co., New York, 1958, pp. 59-61.

18. L. M. Brekhovskikh. Waves in Layered Media, Academic Press, Inc., New York, 1960, pp. 474-476.

19. M. A. Pedersen, D. F. Gordon. Comparison of Curvilinear and Linear Profile Approximation in the Calculation of Underwater Sound Intensities by Ray Theory. J. Acoust. Soc. Amer. 41:419-438, February 1967.

20. U. S. Navy Electronics Laboratory. Technical Memorandum 774(Rev), Performance Prediction Model for Bottom Bounce Operation, by W. H. Watson, 18 February 1965, revised 23 July 1965.

21. U. S. Navy Electronics Laboratory. Technical Memorandum 925, Bottom Bounce Propagation Loss Model I, by W. H. Watson, J. C. Binen, 5 May 1966.

22. Naval Undersea Warfare Center. Technical Note 60, Values of Empirical Expressions for Ambient Sea Noise (U), by H. R. Hall, February 1968, CONFIDENTIAL.

23. R. P. Chapman, J. R. Marshall. Reverberation from Deep Scattering Layers in the Western North Atlantic. J. Acoust. Soc. Amer. 40:405-411, August 1966.

24. W. E. Batzler, R. J. Vent. Volume-Scattering Measurements at 12 kc/sec in the Western Pacific. J. Acoust. Soc. Amer. 41:154, January 1967.

25. R. P. Chapman, J. H. Harris. Surface Backscattering Strengths Measured with Explosive Sound Sources. J. Acoust. Soc. Amer. 34:1594-1597, October 1962.

26. Naval Undersea Research and Development Center. Technical Note 260, Computed Sea Surface Scattering Strengths as a Function of Frequency and Wind Velocity, by L. P. Berger, June 1969.

27. K. V. Mackenzie. Bottom Reverberation for 530- and 1030-cps Sound in Deep Water. J. Acoust. Soc. Amer. 33:1498-1504, November 1961.

28. W. H. Watson. Reverberation as a Factor Affecting Sonar System Effective-
    ness (U), Presented at 7th U. S. Navy Symposium on Military Oceanography.
    Annapolis, Maryland, 12-14 May 1970, CONFIDENTIAL.

29. Naval Oceanographic Office. Informal Report 69-38, Bottom Reverberation
    Measurements in the Norwegian Sea and North Atlantic Ocean, by P. B.
    Schmidt. March 1969.

30. Headquarters Naval Material Command. Principles and Applications of
    Underwater Sound, 1968, p. 193. (Originally Summary Technical Report
    of Division 6, NDRC vol 7.)

31. Naval Undersea Research and Development Center. Technical Note 381,
    Derivation of Cumulative Multi-Ping Detection Probability Model, by
    L. K. Arndt, January 1970.